Pramana – J. Phys. (2021) 95:145
https://doi.org/10.1007/s12043-021-02179-w

Design and analysis of broadband supercontinuum generation in highly nonlinear $LiGaSe_2$-based photonic crystal fibre

MONIKA KIRORIWAL* and POONAM SINGAL

Electronics & Communication Department, Deenbandhu Chhotu Ram University of Science & Technology, Sonepat 131 039, India
*Corresponding author. E-mail: k.kiroriwal@gmail.com

MS received 4 January 2021; revised 22 April 2021; accepted 26 April 2021

Abstract. A numerical investigation of $LiGaSe_2$-based photonic crystal fibre for broad supercontinuum spectrum at − 30 dB intensity level has been studied in this paper. The proposed structure is simulated by the finite element method and provides a zero-dispersion wavelength of 2.46 μm. Higher-order dispersion coefficients are considered to generate a supercontinuum spectrum spanning 2.15–14.6 μm. An input pulse of 30 fs is injected into a small-length photonic crystal fibre with a low input power of 600 W at a pump wavelength of 2.5 μm. This mid-infrared broad spectrum has potential applications in optical coherence tomography, spectroscopy and medical bio-imaging field.

Keywords. Nonlinear optics; photonic crystal fibre; nonlinearity; finite element method; chromatic dispersion.

PACS Nos 42.65.–k; 42.65.Wi; 42.81.Qb

1. Introduction

Photonic crystal fibres (PCFs) are getting more attention in the photonics field for the growth of the mid-infrared supercontinuum (SC) spectrum [1]. Supercontinuum generation (SCG) is a phenomenon that expands an energy pulse while propagating through an optically nonlinear medium. This magical process was first introduced by Alfano and Shapiro [2,3]. Linear characteristics like chromatic dispersion and nonlinear characteristics like self-phase modulation (SPM), cross-phase modulation (XPM), four-wave mixing (FWM), stimulated Raman scattering (SRS) and soliton dynamics are the soul of this SCG process [4]. Due to high absorption loss in the mid-infrared range (MIR), conventional silica-based PCFs have limitations in enhancing the SC spectrum's bandwidth. Nonlinear material-based photonic crystal fibre has a great potential to overcome these limitations. Chalcogenide glasses and other nonlinear optical materials like tellurite, fluoride and nematic liquids are the most attractive for the SC spectrum at longer wavelengths [5,6]. These materials are doped (infiltrated) in the core or cladding region to enhance the optical properties of the existing fibre.

The most commonly used region in the infrared spectroscopy is the mid-infrared region since molecules can soak up radiations in this regime to set off vibrational excitation of effective groups. These vibrational transitions of a molecule have been of immense importance to scientific researchers in diverse fields [7]. Towards this, PCF infiltrated with nonlinear material generates broad spectra expanding from the near to mid-infrared region.

The selected materials must have a wide transparency window with low absorption losses, high linear and nonlinear refractive indices and high thermal stability [8]. Several numerical investigations have been done on silica, bismuth [9,10] and tellurite [11] microstructured fibres. Huan *et al* [12] investigated a broadband SCG spectrum with a bandwidth of 2900 nm in a 5 cm long tellurite-based PCF. Saini *et al* [13] presented a theoretical and numerical computation of SC spectra covering 1.2–15 μm using spiral PCF. Xing *et al* [14] have done simulations to study the generation of SC at –20 dB intensity level in a PCF with 2 cm length. A wide SCG spectrum with a bandwidth of 3.7 μm was presented in a 10 mm PCF by Balani *et al* [15]. Chromatic dispersion and higher-order dispersion (HOD) have significant impact on spectral broadening. In this context, Karim *et al* have numerically studied the influence of HOD on spectra in As_2Se_3-based PCF [16]. A new PCF approach with multimaterial is displayed which generated a wide spectrum covering 1.6–4.2 μm

Published online: 26 August 2021

at 2.5 μm [17]. An $AsSe_2$–As_2S_5-based PCF has been reported to analyse coherent SCG by Diouf *et al* [18]. Vyas *et al* investigated a 100 mm long chalcogenide PCF generating SC spectra spanning 1–15 μm [19]. Dispersion engineering is applied to achieve a desirable flat dispersion profile. Diouf *et al* [20] exhibited an $As_{38.8}Se_{61.2}$-based PCF to generate a 3 dB flat-top coherent SC spectrum spanning 2.9–4.57 μm. A 10 mm long Ge–As–Se-based PCF has been proposed for broadband SC spectra covering 1–16 μm mid-infrared region [21]. Salem *et al* have performed simulations in a 4 mm long multimaterial PCF to achieve a wide SC spectrum (1–5 μm) with 8 dB flatness [22]. Pumped with an all-normal dispersion regime, Medjouri *et al* have investigated and analysed a coherent SC spectrum by applying a laser pulse of 50 fs width with a power of 20 kW in a 1 cm long Ga–Sb–S-based PCF [23]. Chauhan *et al* have demonstrated a 10 mm multicomponent chalcogenide-based PCF to generate continuum spectra extending from 2 to 11 μm [24].

There are various fields, including biomedicine, optical telecommunication, free-space communication, signal security and integration, imaging, sensing and spectroscopy [25–30] where broad SC spectrum is a desirable condition.

In 2016, Vyas *et al* explored the highly nonlinear chalcogenide material $LiGaSe_2$ for SC spectra generation [31]. This wide band-gap (3.34 eV) [32] material can be integrated with heavy metals. It can convert laser radiation to the transparent MIR [33,34]. Lithium-based glass material is less toxic than arsenic-based glass material. These properties make $LiGaSe_2$ appropriate for the MIR applications over the transparency window from 0.5 to 14 μm [35].

The introduction section is followed by §2, which describes the proposed PCF structure. In §3, a numerical study of SC spectrum is given and the results are analysed and compared with the published article's PCF in table 1 in §4, followed by conclusion in §5.

2. PCF design model

A cross-sectional image of the proposed regular hexagonal photonic crystal fibre (PCF) is presented in figure 1a. The numerical computation is performed using commercial finite-element method-based FIMMWAVE software. All equal circular air holes are arranged in a triangular pattern, and the central air hole is missing to concentrate the light in the core area. The perfectly matched layer (PML) is used as an absorbing layer to reduce the unavoidable leakage from the cladding region. Distance between the two holes (centre to centre) is 2.5 μm, known as pitch or lattice-period (Λ). Lithium-based ternary compound ($LiGaSe_2$) is proposed as the host material in place of fused silica. A high nonlinear coefficient can be achieved due to the high nonlinear refractive index of the proposed $LiGaSe_2$ [34]. With the ease of PCF geometry, it can be easily fabricated using a conventional method like stack and draw technique [36] and modern methods like sol–gel technique, mechanical drilling [37,38]. Figure 1b presents the simulated fundamental mode electric field distribution at 2.5 μm.

3. Numerical method for spectrum analysis

Initially, a hyperbolic secant pulse is launched at the starting end of the PCF. This pulse is characterised by the following equation [39]:

$$A(z=0,t) = \mathrm{sqrt}(P_0)\,\mathrm{sech}\left(\frac{t}{T_0}\right) \tag{1}$$

where $T_0 = T_{\mathrm{FWHM}}/1.763$ is the input pulse width and P_0 is the pulse peak power. A refers to the pulse envelope at zero distance and T_{FWHM} indicates the full-width at half-maximum.

Linear and nonlinear dynamics-based SCG process is analysed using the nonlinear Schrödinger equation (NLSE) [39].

$$\frac{\partial A}{\partial z} + \frac{\alpha}{2}A - \left(\sum_{n\geq 2}\beta_n \frac{i^{n+1}}{n!}\frac{\partial^n A}{\partial t^n}\right) = i\gamma\left(1 + \frac{i}{\omega_0}\frac{\partial}{\partial t}\right) \times \left[A(z,t)\int_{-\infty}^{\infty} R(t')\left\lfloor A(z,t-t')\right\rfloor^2 \mathrm{d}t'\right]. \tag{2}$$

Left-hand side (LHS) of eq. (2) signifies the linear effect and right-hand side (RHS) signifies the nonlinear effects at pumped angular frequency ω_0. The parameter α is the attenuation coefficient and $\beta_n = \mathrm{d}^n\beta/\mathrm{d}\omega^n$ indicates higher-order dispersion coefficients up to nth order as described in eq. (3) [39]. The nonlinear coefficient is denoted by γ. $A(z,t)$ represents the output signal envelope. $R(t')$ denotes the nonlinear Raman response characterised by eq. (4).

The Taylor series expansion for β_n is

$$\beta(\omega) = \beta(\omega_0) + \beta_1(\omega_0)(\omega-\omega_0) + \frac{1}{2!}\beta_2(\omega_0)(\omega-\omega_0)^2 + \cdots. \tag{3}$$

The first term of the RHS is the effective refractive index of the confined mode, the second term denotes group velocity and the third term represents group velocity dispersion of the propagating pulse [29].

$$R(t') = (1-f_{\mathrm{R}})\delta t + f_{\mathrm{R}}h_{\mathrm{R}}(t), \tag{4}$$

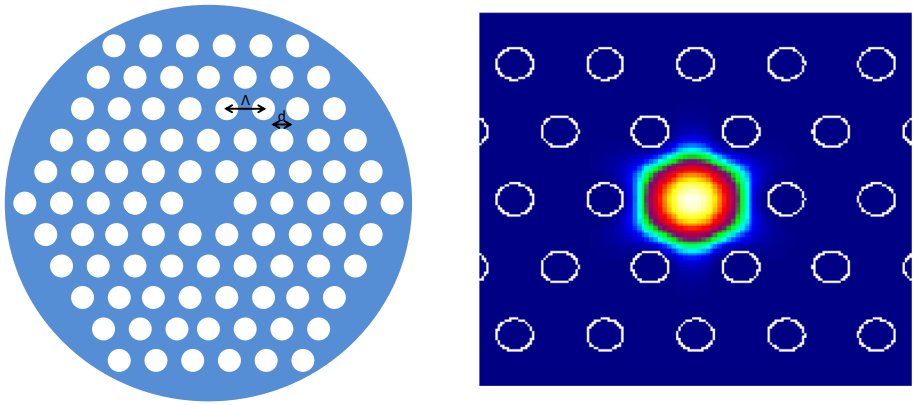

(a) (b)

Figure 1. (**a**) Transverse view of PCF geometry and (**b**) confined electric field distribution at 2.5 μm.

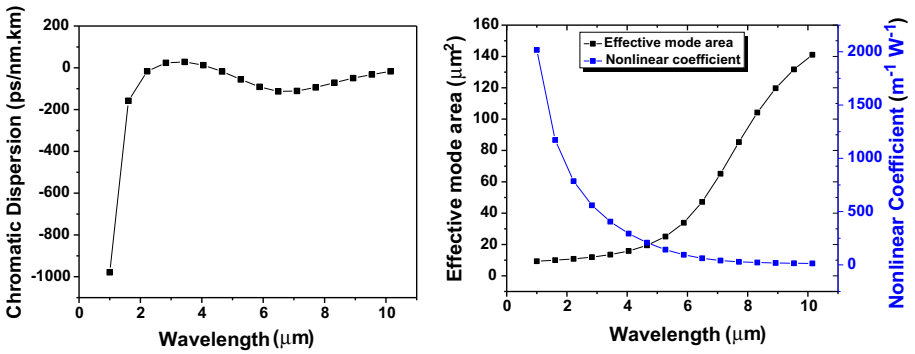

(a) (b)

Figure 2. (**a**) Chromatic dispersion characteristics and (**b**) effective mode area and nonlinear coefficient as a function of the operating wavelength.

where f_R is Raman response's fractional contribution and $h_R(t)$ displays Raman response function expressed by [30]

$$h_R(t) = \frac{\tau_1^2 + \tau_2^2}{\tau_1 \tau_2^2} \exp\left[-\frac{t}{\tau_2}\right] \sin\left(\frac{t}{\tau_1}\right). \tag{5}$$

Raman response function includes Raman period τ_1 and damping time τ_2. For the generation of continuum spectra f_R =0.115, τ_1 =23.1 fs and τ_2 =195 fs of As_2Se_3 are considered [40].

Equation (2) has a combined effect of linear and nonlinear characteristics of PCF. Dispersion arises due to velocity differences during linear propagation of pulse. Wavelength-dependent material dispersion and linear refractive index are calculated using Sellmeier's formula [31]

$$n(\lambda) = \text{sqrt}\left(A + \frac{B}{\lambda^2 - C} + D\lambda^2\right), \tag{6}$$

where $A = 5.22442$, $B = 0.18365$, $C = 0.07493$, $D = 0.00232$ and λ is an operating wavelength in micrometres for the proposed nonlinear material $LiGaSe_2$. Material is employed after defining the refractive index according to eq. (6) in available FIMMWAVE. The chromatic dispersion (CD) is determined using the relation [3]

$$\text{CD}(\lambda) = -\frac{\lambda}{c}\frac{\text{d}^2 n_{\text{eff}}}{\text{d}\lambda^2} (\text{ps/nm·km}). \tag{7}$$

Nonlinear behaviour is accounted for on the basis of nonlinear coefficient (γ), which is calculated by [4]

$$\gamma = \frac{2\pi n_2}{\lambda A_{\text{eff}}(\lambda)} (\text{m}^{-1}\,\text{W}^{-1}), \tag{8}$$

where $n_2 = 3 \times 10^{-15}\,\text{m}^2/\text{W}$ is the nonlinear refractive index of the host material [34]. Effective mode area A_{eff} is estimated using the electric field distribution of the confined mode [3]

$$A_{\text{eff}}(\lambda) = \frac{\left(\int\int_{-\infty}^{\infty} |E|^2 \text{d}x\text{d}y\right)^2}{\left(\int\int_{-\infty}^{\infty} |E|^4 \text{d}x\text{d}y\right)} (\mu\text{m}^2) \tag{9}$$

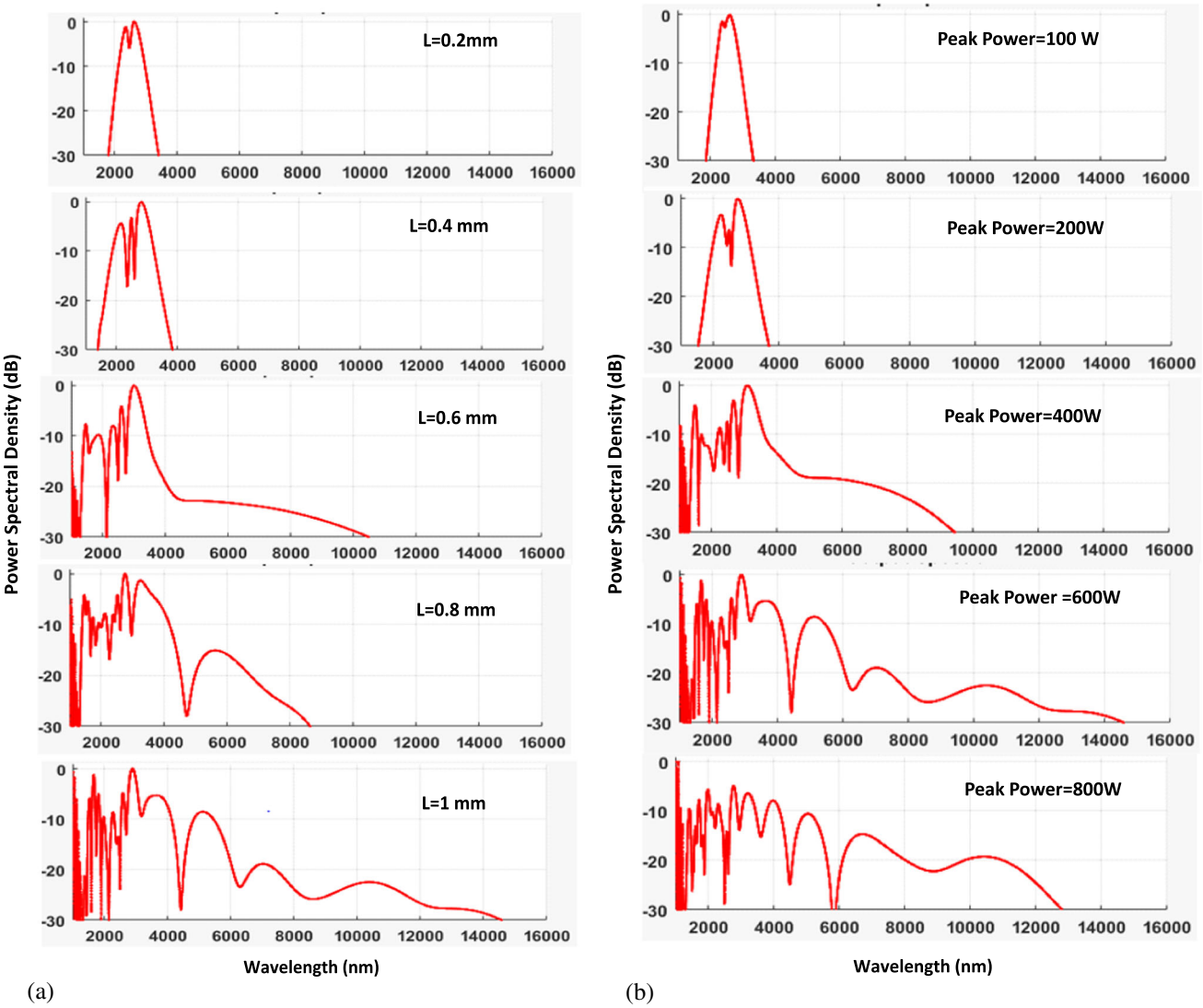

Figure 3. (**a**) Influence of different fibre length with fixed pulse parameters and (**b**) influence of different input peak power with stable pulse width and fixed fibre length on the broadening of supercontinuum spectrum.

The effective mode area can be minimised by utilising the design flexibility feature of the PCF. A small effective area has a significant impact on the nonlinear behaviour of the existing fibre.

4. Results and analysis

4.1 *Linear and nonlinear characteristics*

Linear and nonlinear properties of the host material greatly impact the optical properties of the PCF [39]. Dispersive behaviour is a significant parameter that directly affects the nonlinear interplay of the structured fibre. The dispersion process is proportionally related to the effective mode refractive index [3]. A number of iterations have been executed to get effective optical parameters to generate a SC spectrum. The chromatic dispersion characteristics are shown in figure 2a. Material and waveguide dispersion is zero at 2.46 μm, known as zero-dispersion wavelength (ZDW). 2.5 μm is adapted as the pump wavelength to transfer maximum energy for soliton dynamics. Minimum dispersion of 3.16 ps/nm·km is found at the pump wavelength. The variation in the effective mode area and nonlinear coefficient for the effective PCF's parameters at different mid-infrared wavelengths are shown in figure 2b. The effective mode area exponentially increases from 9.34 to 140 μm^2 due to the unavoidable light leakage in the cladding region.

Effective mode area and nonlinear refractive index play crucial roles in enhancing the nonlinearity of the PCF [3]. The designed PCF possesses very high nonlinear coefficient (661.05 $m^{-1} W^{-1}$) at 2.5 μm pump wavelength. This high value of nonlinearity makes it a suitable candidate for SC generation.

5. Analysis of supercontinuum spectrum

Supercontinuum spectrum is a broad white spectrum, which is the combined result of linear and nonlinear characteristics of the PCF as expressed by eq. (2). Input pulse width, peak power and fibre length (L) are control parameters for spectrum broadening. We have analysed and reported the effects of each parameter on the SC process. Split-step Fourier method (SSFM) using MATLAB is used for solving nonlinear differential equations [38].

SC spectrum is a plethora of nonlinear impairments like SPM, XPM, FWM and SRS [4]. SPM and XPM are liable for the initial phase of a broad spectrum. When a high-intensity femtosecond (fs) pulse is applied on a highly nonlinear fibre, the intensity-dependent refractive index leads to SPM. Due to minimum dispersion at pump wavelength, there is a symmetrical spectral broadening with the same input pulse envelope [21]. Further broadening occurs due to XPM because more than one optical field simultaneously propagate in the confined area. FWM arises due to the third-order Kerr nonlinearity, and there is an interaction of pulses to generate new photons at new frequencies. Phase-matching conditions should be satisfied to complete this interaction [27].

The effects of pulse parameter and fibre length on the SC spectrum have been analysed after injecting a secant hyperbolic pulse with a duration of 30 fs and peak power of 600 W. Fibre length is varied from 0.2 mm to 1 mm, and the obtained spectra are presented in figure 3a. Due to the very high nonlinear coefficient, the calculated fibre length is very small. As the optical pulse propagates in the core area, it may be dominated by dispersive or nonlinear effects like SPM, followed by XPM, FWM and SRS [4]. A high-intensity electric field interacts with dielectric media throughout the fibre length leading to a pulse broadening. Up to 1 mm fibre length, the entire broadening process has been completed. Beyond 1 mm fibre length, the pulse experiences signal losses instead of broadening.

Input peak power is also an effective controlling parameter. We have analysed the influence of pulse peak power from 100 to 600 W while pulse duration (30 fs) and fibre length (1 mm) are fixed, as displayed in figure 3b. When peak power is increased up to 600 W, the output spectrum broadens due to the increased stoke wave generation at longer wavelengths [28]. Further, at 800 W peak power, there is pulse compression and and reduction in spectrum bandwidth. The SC spectrum bandwidth covers 2.15–14.6 μm, after applying the hyperbolic secant pulse of 30 fs pulse width with 600 W peak power in 1 mm proposed PCF.

Pulse width also plays an essential role in the generation of an SC spectrum [41]. The effect of variation in the pulse duration from 30 to 90 fs with a gap of 20 fs on the SC spectrum has been reported in this 1 mm long PCF with 600 W pulse peak power as illustrated in figure 4. The changing rate of intensity varies with applied pulse duration and affects the nonlinear interaction between input pulse and dielectric media [27]. Due to this interaction, at the first stage, SPM occurs followed by other nonlinear processes resulting in a broader spectrum. It is clearly shown in figure 4 that the SC broadening reduces while pulse width increases.

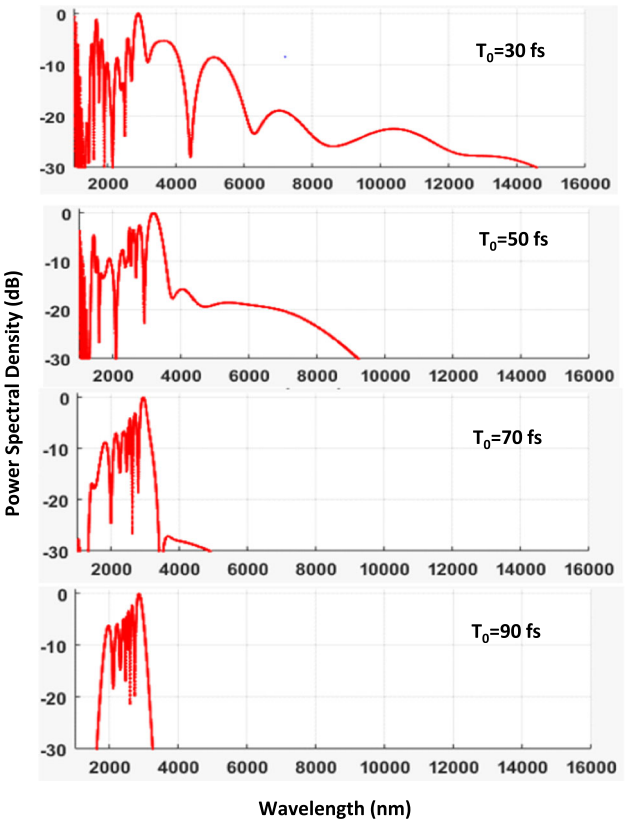

Figure 4. Influence of different pulse width (30 fs, 50 fs, 70 fs and 90 fs) on SC spectra when the peak power is 600 W.

6. Conclusion

A regular design of highly nonlinear $LiGaSe_2$ hexagonal PCF is introduced for high bandwidth MIR SC spectrum. The investigated geometry provides an ultrahigh nonlinearity of 661.05 m^{-1} W^{-1} with a small effective area at an exciting wavelength of 2.5 μm. In the designed 1 mm long PCF, an SC spectrum with a high bandwidth of 12.45 μm has been acquired at -30 dB intensity level by injecting a 30 fs pulse with 600 W peak power. This power-efficient broad SC spectrum has applications in many nonlinear optical fields, including fibre laser, frequency comb generation, wavelength conversion, sensing and vital disease detection [7,42–45].

Table 1. SCG in the designed PCF compared with the article's reported PCFs.

PCF design	Pump wavelength (μm)	PCF length	SC spectrum (μm)
$60TeO_2$–20PbO–$20PbCl_2$-based PCF [12]	2.45	5 cm	2–4.9
$As_{38.8}Se_{61.2}$ PCF [20]	3.7	5 cm	2.9–4.575
As_2S_5–borosilicate PCF [22]	2.5	4 mm	1–5
$Ga_8Sb_{32}S_{60}$ PCF [23]	4.5	1 cm	1.65–9.24
$GeSe_2$–As_2Se_3–PbSe PCF [24]	3.1	10 mm	1–11
Proposed $LiGaSe_2$-based PCF	2.5	1 mm	2.15–14.6

References

[1] J M Dudley and J R Taylor, *Nature Photon.* **3**, 85 (2009)
[2] R R Alfano and S L Shapiro, *Phys. Rev. Lett.* **24**, 584 (1970)
[3] P S J Russell, *J. Lightwave Technol.* **24**, 4729 (2006)
[4] J M Dudley, G Genty and S Coen, *Rev. Mod. Phys*. **78**, 1135 (2006)
[5] J M Dudley and J R Taylor, *Supercontinuum generation in optical fibres* (Cambridge University Press, 2010)
[6] J S Sanghera, C M Florea, L B Shaw, P Pureza, V Q Nguyen, M Bashkansky, Z Dutton and I D Aggarwal, *J. Non-Cryst. Solids* **354**, 462 (2008)
[7] T S Saini, A Kumar and R K Sinha, *J. Lightwave Technol.* **33**, 3914 (2015)
[8] J Hu, C R Menyuk, L B Shaw, J S Sanghera and I D Aggarwal, *Opt. Express* **18**, 6722 (2010)
[9] J Gopinath, H Shen, H Sotbayashi, E Ippen, T Hasegawa, T Nagshima and N Sugimoto, *Opt. Express* **12**, 5697 (2004)
[10] R Buczynski, H T Bookey, M Klimczak, D Pysz, R Stepien, T Martynkien, J E McCarthy, A J Waddie, A K Kar and M R Taghizadeh, *Materials* **7**, 4658 (2014)
[11] P Domachuk, N A Wolchover, M Cronin-Golomb, A Wang, A K George, C M B Cordeiro, J C Knight and F G Omenetto, *Opt. Express* **16**, 7161 (2008)
[12] T Huang, P Huang, Z Cheng, J Liao, X Wu and J Pan, *Opt. Int. J. Light Electron Opt.* **167**, 144 (2018)
[13] T S Saini, A Bailli, A Kumar, R Cherif, M Zghal and R K Sinha, *J. Mod. Opt.* **62**, 1570 (2015)
[14] S Xing, S Kharitonov, J Hu and C-S Brès, *Opt. Express* **26**, 19627 (2018)
[15] H Balani, G Singh, M Tiwari, V Janyani and A K Ghunawat, *Appl. Opt.* **57**, 3524 (2018)
[16] M R Karim, H Ahmad, S Ghosh and B M A Rahman, *Opt. Fibre Technol.* **45**, 255 (2018)
[17] S Kalra, S Vyas, M Tiwari and G Singh, Multi-material photonic crystal fibre in MIR region for broadband supercontinuum generation, in: *Optical and wireless technology* (Springer, 2018) p. 199
[18] M Diouf, A Wague and M Zghal, *J. Opt. Soc. Am. B* **36**, A8 (2018)
[19] S Vyas, T Tanabe, M Tiwari and G Singh, *Chin. Opt. Lett.* **14**, 123201 (2016)
[20] M Diouf, A B Salem, R Cherif, H Saghaei and A Wague, *Appl. Opt.* **56**, 163 (2017)
[21] A G N Chaitanya, T S Saini, A Kumar and R K Sinha, *Appl. Opt.* **55**, 10138 (2016)
[22] A B Salem, M Diouf, R Cherif, A Wague and M Zghal, *Opt. Eng.* **55**, 066109-1- (2016)
[23] A Medjouri, D Abed and Z Becer, *Opto-Electron. Rev.* **27**, 1 (2019)
[24] P Chauhan, A Kumar and Y Kalra, *Opt. Fibre Technol.* **54**, 102100 (2020)
[25] S Dupont, C Petersen, J Thøgersen, C Agger, O Bang and S R Keiding, *Opt. Express* **20**, 4887 (2012)
[26] T S Saini, N P T Hoa, T H Tuan, X Luo, T Suzuki and Y Ohishi, *Appl. Opt.* **58**, 415 (2019)
[27] P Chauhan, A Kumar and Y Kalra, *Opt. Int. J. Light Electron Opt.* **187**, 92 (2019)
[28] P Chauhan, A Kumar and Y Kalra, *Opt. Fibre Technol.* **46**, 174 (2018)
[29] M R Karim, B M A Rahaman and G P Agrawal, *Opt. Express* **23**, 6903 (2015)
[30] T S Saini and U S Tiwari, *J. Appl. Phys.* **122**, 053104-1 (2017)
[31] S Vyas, M Tiwari, T Tanabe and G Singh, *Proceedings of the International Conference on Recent Cognizance in Wireless Communication & Image Processing* (Springer, 2016) p. 409
[32] F Liang, L Kang, Z Lin and Y Wu, *Cryst. Growth Design* **17**, 2254 (2017)
[33] L Isaenko, A Yelisseyev, S Lobanov, A Titov, V Petrov, J J Zondy, P Krinitsin, A Merkulov, V Vedenyapin and J Smirnova, *Cryst. Res. Technol.* **38**, 379 (2003)
[34] V Vedenyapin, L Isaenko, A Yelisseyev, S Lobanov, A Tyazhev, G Marchev and V Petrov, *Proc. SPIE* **7917**, 1 (2011)
[35] A Yelisseyev, F Liang, L Isaenko, S Lobanov, A Goloshumova and Z S Lin, *Opt. Mater.* **72**, 795 (2017)
[36] E Issa, M A Eijkelenborg, M Fellew, F Cox, G Henry and M C Large, *Opt. Lett.* **29**, 1336 (2004)
[37] R T Bise and D Trevor, Sol-gel derived micro structured fibers: Fabrication and characterization, in: *Proceedings of the Optical Fibre Communication Conference (OWL6)* (2005)
[38] P Zhang, J Zhang, P Yang, S Dai, X Wang and W Zhang, *Opt. Fibre Technol.* **26**, 176 (2015)
[39] G P Agrawal, *Nonlinear fibre optics*, 5th Edn (Academic Press, San Diego, California, 2013)
[40] B Ung and M Skorobogatiy, *Opt. Express* **18**, 8647 (2010)

[41] A A Nair and M Jayaraju, *Pramana – J. Phys.* **91**: 66 (2018)
[42] U Chakravarty, A Kuruvilla, R Singh, B N Upadhyay, K S Bindra and S M Oak, *Pramana – J. Phys.* **82**, 379 (2014)
[43] L Li, N Abdukerim and M Rochette, *Opt. Lett.* **42**, 639 (2017)
[44] J Yuan, Z Kang, F Li, X Zhang, X Sang, Q Wu, B Yan, K Wang, X Zhou, K Zhong, G Zhou, C Yu, C Lu and H Y Tam, *J. Light Wave Technol.* **35**, 2994 (2017)
[45] M L Ferhat, L Cherbi and I Haddouche, *Opt. Int. J. Light Electron Opt.* **152** 106 (2018)